URSI GASS 2020, Rome, Italy, 29 August - 5 September 2020

An orientation-independent UHF battery-less Tag for extended-range Applications

D. Fabbri(1), A. Romani(1), A. Costanzo(1), and D. Masotti(2)
(1) DEI-ARCES – University of Bologna, Cesena, Italy
(2) DEI – University of Bologna, Bologna, Italy

Abstract

This paper describes the architecture and design criteria of a double monopole, battery-less, individually addressable RF tag for all those applications where long working distances are required (objects localization, environmental sensing, etc.). The prototype is built with off-the-shelf components in a 92x95 mm^2 PCB design through low losses Rogers 4350 substrate. The proposed circuit implements two rectennas orthogonally oriented combined with matching and decoupling networks which guarantee a low-directive behavior for an orientation-independent usage of the tag. A micro-power management unit supplies the on-board ultra-low power circuitry. The node can power-up from a fully-discharge state with a 2W ERP source in the UHF 865-868 MHz band at 12 m of distance and operates at a maximum distance of 21.9 m with a sensitivity of -21 dBm.

1 Introduction

The world of the Internet of Things (IoT) combined with wireless machine to machine communication (M2M) [1] where objects talk to each other, make decision autonomously and sense the environment in support of humans, enables advanced services, by justifying the rapid increase of the number of smart devices connected to Wireless Sensor Networks (WSNs). In this context, the use of energy harvesting techniques to supply devices, nowadays, plays an important role in order to create energy autonomous systems able to reduce the use of batteries, by containing the infrastructure maintenance costs, for better environmental safeguard.

Hence, (RF) energy-scavenging has been highly investigated during the recent years [2][3]. Such kind of systems can work in harsh environments with non-line of sight conditions between transmitters and objects extending the number of applications in which this technology can be adopted (logistics, tracking of goods, environmental sensing, etc.) [4][5]. In general, passive UHF tags can work with a read-range of few tens of meters [6] thanks to the high sensitivity of commercial RF transceivers available in the market: Monza X 2K [7], Higgs 4 [8] and others [5]. Several RF battery-less tag solutions have been presented in the academic field, starting from the Wireless Identification and Sensing Platform (WISP), in 2007 [9] and 2008 [10] developed by P. Sample et. al., which was able to work up to 4.5 m from the RF source with a single dipole antenna. In the recent years, a newest micropower design of UHF battery-free node has been presented in 2018 [11] which fully operates up to 10.80 m with a single monopole antenna. Subsequently, the circuit has been integrated with EPC Gen 2 standard in 2019, through a microcontroller based flexible platform by maintaining the same working distances [12]. The performances of these solutions are affected by the tag orientation with respect to the transmitter due to the presence of a single linearly-polarized antenna. For this reason, a multi-element antenna was designed in 2019 [13] to facilitate the increase of working distances for all possible tag orientations and positions, improving the communication stability of the wake-up radio (WUR) and the energy harvesting chain.

The aim of this work is to integrate the base-band circuits designed in [11] with a multi-element antenna [13], specifically developed to overcome issues related to the tag orientations, besides improving the system stability and the rectifier available power for wider working distances.

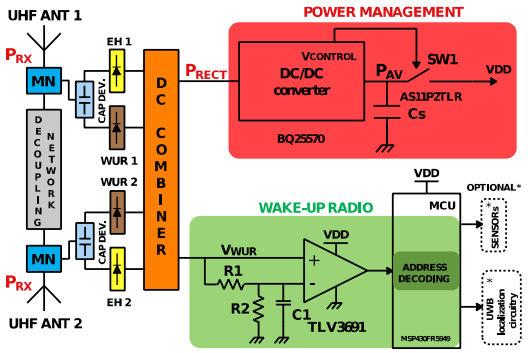

Figure 1. Architecture of the proposed double monopole UHF passive tag.

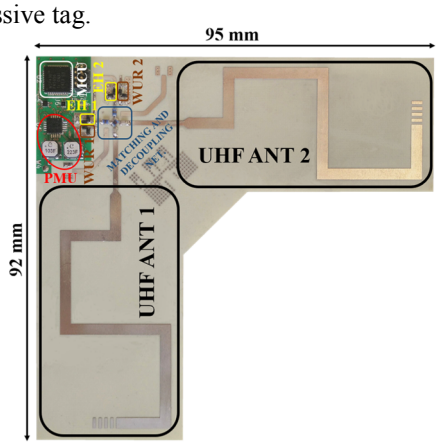

Figure 2. Double monopole UHF passive tag PCB board.

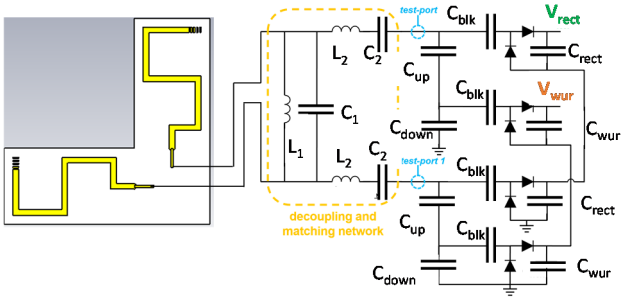

Figure 3. Schematic view of the two-monopole rectenna.

Table I. Lumped components values.

L_1 (Coilcraft)	56 nH	**C_{down}** (Murata)	1 pF
C_1 (Murata)	2.8 pF	**C_{blk}** (ATC)	10 pF
L_2 (Coilcraft)	27 nH	**C_{rect}** (Murata)	10 pF
C_2 (Murata)	39 pF	**C_{wur}** (Murata)	10 pF
C_{up} (Murata)	0.7 pF		

2 Tag hardware design

The hardware architecture of the proposed passive tag is depicted in Fig. 1. It is based on two UHF meandered monopoles, combined with a matching and decoupling network studied to maximize the rectified power, firstly, for energy harvesting and secondly for Wake-up radio purposes. Hence, the node implements a DC/DC converter unit in order to manage the incoming energy and make it available for the WUR module. It integrates a data slicer used to clean the received addresses combined with an ultra-low-power MCU used for comparing the incoming bit-stream with the locally stored tag address.

Optional UWB localization circuitry [11][14] and low power sensors [12] can be easily integrated on-board and managed by the MCU as additional tasks, allowing to serve a wide range of applications [4][5]. The prototype board is built-in a low-losses Rogers 4350 RF substrate with 4 layers PCB technology (Fig.2).

2.2 Double-monopole rectenna

The rectifying antenna (rectenna) part of the tag is a delicate design task, especially if UHF frequency is involved, thus forcing large footprint to the radiating section. This is true for tags that usually need for compact size, in particular when the number of adopted antennas is greater than one, as for the present project, where an orientation-independent behavior of the rectenna is envisaged [13]. Fig. 3 shows the schematic view of the double rectenna architecture: two meandered monopoles with orthogonal orientation are used as receiving antennas, hence able to capture any polarized incoming field. The most interesting feature of the radiating part relies on the close proximity of the two antennas (in order to maintain the overall tag dimension within 9.5 x 9.2 cm^2): for energy harvesting purposes, it is important to guarantee an omnidirectional behavior of the two rectennas, and this is obtained by including a lumped

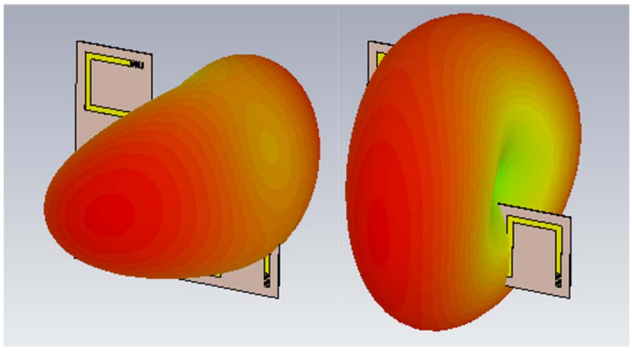

(a) (b)

Figure 4. Radiation pattern of the horizontal monopole: (a) in absence, (b) in presence of the decoupling network.

element network, in between antennas and rectifiers, acting both as a matching and as a decoupling network.

The effectiveness of the decoupling network is numerically demonstrated in Fig. 4, where the radiation pattern of the horizontal monopole is shown, in absence (Fig. 4(a)) and in presence (Fig. 4(b)) of the decoupling network: in the second case, the radiation pattern is almost undistorted, showing that the monopole is radiating as if it were isolated from the other monopole. Moreover, the effects of the electromagnetic coupling are not only related to the radiation properties (shown in Fig. 4), but also to the signal distribution in the circuit, which is definitely unpredictable.

Another distinctive feature of the tag under test is represented by the dual path rectifying section (per each antenna). There are two voltage doublers (with Skyworks SMS 7630 Schottky diodes) derived in parallel from the decoupling network path: one provides the main rectifying operation, the other spills a small portion of the signal for WUR operation. The signal splitting is made more effective by resorting to a fully-reactive partition network (with C_{up} and C_{down} capacitors) that guarantees almost no losses if compared to a resistive one. The two rectenna outputs are then combined in series to maximize the overall rectified voltage. Table I reports the values of the lumped components of Fig. 3.

The main goal when designing the rectifying section has been to maintain the highest main rectified voltage (V_{rect}) when changing, as in real operating conditions, the load offered by the WUR: if the available input power provided to a single monopole is -13 dBm and the WUR load changes from 0.1 to 100 kΩ, V_{rect} remains around 900 mV [13].

As a preliminary test the dual-monopole architecture has been compared with a single-monopole one by

Table II. Open circuit dc voltage for the single- and the double-monopole rectennas in vertical and oblique orientations.

	Single	**Double**
V	400 mV	930 mV
O	320 mV	915 mV

measuring the open-circuit rectified voltage at their dc output ports (before connecting the PMU described in the following section). A circularly-polarized patch antenna sends a UHF power corresponding to -13 dBm in the rectennas location: in this way, each monopole receives -16 dBm. The corresponding results are reported in Table II for two representative orientations: a vertical orientation for the single monopole and for one of the double-monopole case (V), an oblique orientation corresponding to a 45° right rotation of the previous one (O). More than double rectification is achieved in both cases by the multi-rectenna architecture.

2.3 Power Management

Once the incoming power (P_{RX}) is rectified by both rectennas, most of the energy is provided to the power management unit through an unbalanced capacitor divider. The PMU is composed of a buck-boost converter (TI bq25570) able to start-up with 15 µW as input power and 330 mV of input voltage. After the cold-start operation, the main converter is enabled and sets the regulated output voltage to 2.1 V.

Since the device is specifically developed for energy-scavenging purposes it implements the maximum power point tracking (MPPT) of the input sources and integrates a voltage monitor which enables the load, by driving SW1, only when the storage voltage rises over a certain threshold (VH=2.6 V) and disconnects it under the lower threshold (VL=2 V). The use of the load power gating preserves the state of charge of the storage capacitor when the supply voltage is not sufficient to sustain the wake-up radio circuit, in order to have faster re-charge time.

It is worth mentioning that a good practice for minimizing the overall power consumption is to set the lower threshold at the minimum voltage supply required by the load and define a small hysteresis between upper and lower thresholds voltages (compatible with the energy consumption required by the application). Moreover, a smart choice of the storage capacitor (Cs) has to be done considering the amount of energy required to operate. Therefore, having large values of capacitance can help to execute more energy-intensive tasks with the disadvantage of longer recharge times (besides the high initial start-up time). In this case, the best trade-off was identified in Cs = 15 µF. Thus, considering the previously presented aspects, the node can work in two different modes: *continuous* and *duty-cycle* mode, depending on the amount of the incoming power. As shown in Fig. 5, when the rectified power (P_{RECT}), as input of the PMU, is lower than the average power required by the load to operate (P_{AVG}/η, where η is the efficiency of the DC/DC converter) there is the transition between continuous to duty-cycle mode where the tag needs a recharge time period to recover the energy lost during the addressing phase before the next activation round.

If not enough power is collected ($P_{RECT} < P_{DCDC} = 1.3$ µW, which represents the quiescent power consumption of the PMU) the DC/DC converter itself is not able operate and it slowly discharge the capacitor Cs.

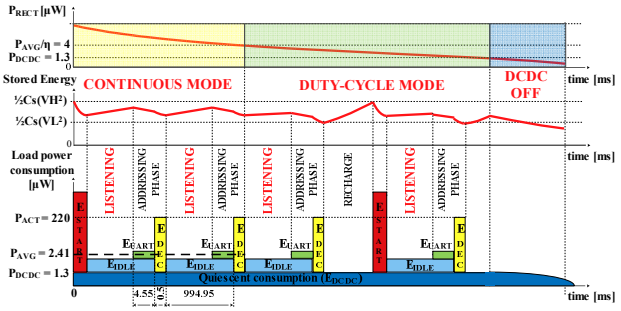

Figure 5. Tag power consumption during continuous and duty-cycle modes referred to the rectified power, for the particular case of one activation per second.

2.4 Wake-up radio

Part of the incoming power is delivered to WUR unit which demodulates an on-off keying (OOK) sequence actuated by the RF source on the UHF-868 MHz carrier frequency (Fig. 1). During an addressing phase the node is in LISTENING state waiting for a bit-stream based on 10-bit word (1 bit start, 8 bit data, 1 bit stop), with a data rate of 2.2 Kbit/sec which is filtered and converted to digital voltage levels through a data-slicer (TLV3691), before being processed by the on-chip UART module of the microcontroller. The serial peripheral is clocked by a very low power oscillator (VLO) at 10 kHz and works while the MCU is in sleep mode to save energy. The CPU is woken-up in ACTIVE state, by an interrupt, only when all the bits are acquired (4.55 ms) and ready to be compared with the initially stored internal identifier (500 µs). In this phase a higher frequency internal digitally controlled oscillator (DC0) is enabled at 1 MHz, which makes the MCU more responsive to end as soon as possible the comparison of bits for generating an external wake-up signal used to test the overall performances.

3 Experimental results

The test bench for measurements implemented in real indoor environment is depicted in Fig. 6. It includes a control interface CI (Raspberry Pi 3) which defines all protocol timings and digital data used to modulate an 868 MHz carrier frequency through the SPIRIT 1 STEVAL-IKR002V4D transceiver board combined with the power amplifier (PA) Qorvo RF6886 and UHF PN6-868RCP-1C circularly-polarized antenna (6 dBi). The total amount of transmitted power is compliant with the European standard (ETSI) and fixed to 2 W ERP. In order

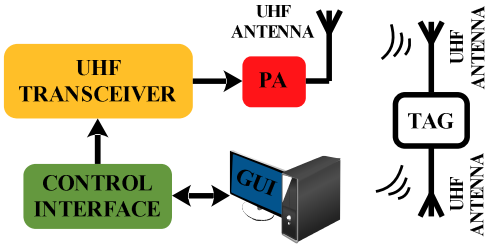

Figure 6. Test bench for measurements.

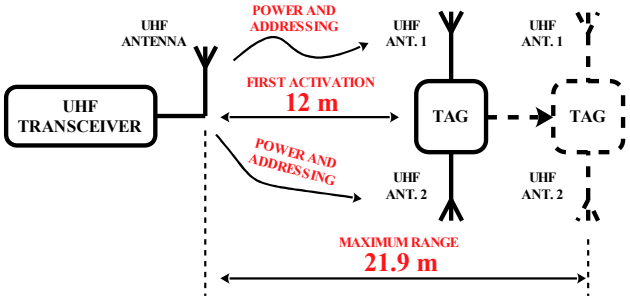

Figure 7. First activation and maximum range of the proposed battery-less node.

Table III. Tag activation rate as a function of the distance.

D [m]	**2**	**4**	**6**	**8**	**10**	**12**
# act.	198 /sec	198 /sec	198 /sec	152 /sec	92 /sec	56 /sec
D [m]	**14**	**16**	**18**	**20**	**21.9**	**22**
# act.	30 /sec	16 /sec	8 /sec	3 /sec	2 /min	0

to simplify the control system operations a Graphical User Interface (GUI) has been developed in MATLAB for setting all parameters and addresses.

First of all, by considering the scenario shown in Fig.7, to characterize the tag performances the double monopole battery-less node is placed away from the transmitter and progressively closer and closer until the main energy converter is powered up, starting from a fully discharge state (first activation at 12 m). Once activated, thanks to lower power consumption required, the node can operate at higher distances up to 21.9 m (with an activation rate of 2 times per minute) as maximum distance from which the DC/DC converter has not enough input power to operate. The activation rate, reported in Tab. III, decreases with the square of the distance (as Friis formula) and shows a saturation up to 6 m of 198 wake-up per second. Since an addressing phase is ended in 5.05 ms (address acquisition and computational time), the data-rate of 2.2 Kbit/sec adopted to identify a tag sets the limit on the maximum number of activations per second.

The tag has been tested in different orientations, with steps of 45°, where no significant performance differences have been recorded, by confirming an orientation-independent behavior of the node in the reported results.

4 Conclusions

The proposed UHF tag solution combines the ultra-low power design of the power management unit to the careful design of two closely-spaced and uncoupled rectennas, thus enabling an effective behavior in indoor environments where the non-ideality of the channel can affect the tag performance. A power-up distance of 12 m and an operating distance of almost 22 m is guaranteed by our promising prototype. The system flexibility, given by the MCU-based WUR, allows an easy integration of indoor localization circuitry [11][14] and low power sensors [12], which makes the platform highly attractive for a wide range of applications with long distance requirements.

5 References

[1] Chen, Min & Wan, Jiafu & Li, Fang, “Machine-to-Machine Communications: Architectures, Standards and Applications”, KSII Transactions on Internet and Information Systems, 2012.

[2] J.A. Hagerty, F.B. Helmbrecht, W.H. McCalpin, R. Zane, Z.B. Popovic, "Recycling ambient microwave energy with broad-band rectenna arrays," IEEE Trans. Microwave Theory and Techniques, 52(3), 2004.

[3] A. Costanzo, F. Donzelli, D. Masotti and V. Rizzoli, "Rigorous design of RF multi-resonator power harvesters," EuCAP, 2010.

[4] P. Adamcova, Z. Tobes, “UHF RFID Technology and its Application”, 17th International Conference Radioelektronika, June 2007.

[5] L. Cui, Z. Zhang, N. Gao, Z. Meng and Z. Li, “Radio Frequency Identification and Sensing Techniques and Their Applications – A Review of the State-of-the-Art”, Sensors, 17 September 2019.

[6] F. K. Byondi and Y. Chung, “Longest-Range UHF RFID Sensor Tag Antenna for IoT Applied for Metal and Non-Metal Objects”, Sensors, 11 Dec. 2019.

[7] Monza X 2K RAIN RFID Tag chip [Online], Available: https://www.impinj.com/.

[8] Higgs 4 RFID IC [online], Available: https://www.alientechnology.com/.

[9] A. P. Sample, D. J. Yeager, P. S. Powledge, J. R. Smith,“Design of Passively-Powered, Programmable Sensing Platform for UHF RFID Systems”, IEEE International Conference on RFID, Grapevine (TX, USA), March 2007.

[10] A. P. Sample, D. J. Yeager, P. S. Powledge, A. V. Mamishev, J. R. Smith, “Design of an RFID-Based Battery-Free Programmable Sensing Platform”, IEEE Transaction on Instrumentation and Measurement, Vol. 57, No. 11, Nov. 2008.

[11] D. Fabbri, M. Pizzotti, and A. Romani, “Micropower Design of an Energy Autonomous RF Tag for UWB Localization Applications”,IEEE ISCAS, May 2018.

[12] D. Fabbri, E. Berthet-Bondet, D. Masotti, A. Costanzo, D. Dardari, A. Romani, “Long Range Battery-less UHF-RFID Platform for Sensor Applcation”, IEEE RFID-TA, September 2019.

[13] M. Fantuzzi, G. Paolini, M. Shanawani, A. Costanzo, D. Masotti, “An Orientation-independent UHF Rectenna array with a Unified Matching and Decoupling RF network”. Int. J. Microwave and Wireless Technologies, 11 (5-6), 2019.

[14] A. Costanzo, D. Dardari, J. Aleksandravicius, N. Decarli, M. Del Prete, D. Fabbri, M. Fantuzzi, A. Guerra, D. Masotti, M. Pizzotti and A. Romani, “Energy Autonomous UWB Localization”, IEEE Journal of Radio Frequency Identification, September 2017.